

COMPACT FINITE DIFFERENCE SCHEMES ON THE CUBED-SPHERE

Jean-Pierre Croisille

Département de mathématiques
Université de Lorraine - Metz, France

Isaac Newton Institute for Mathematical Sciences

September 24, 2012



- 1 The Cubed-Sphere Grid
- 2 One-dimensional Hermitian compact operators on the Cubed-Sphere
- 3 High-order accurate discrete differential operators on the Cubed-Sphere
- 4 Applications

The Cubed-Sphere grid

The cubed-sphere

The Cubed-Sphere is a spherical grid made of six identical squared patches matching the faces of a cube.

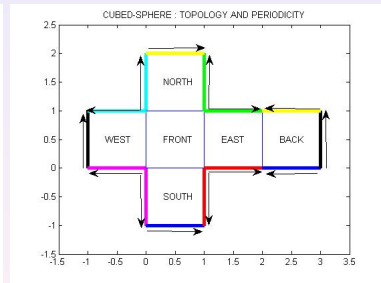
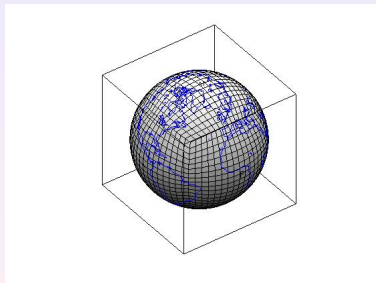


Figure: **Left:** Cubed-Sphere grid. **Right:** Topology and spherical periodicity.

Patch FRONT of the Cubed-Sphere grid

Equiangular coordinate system

On each patch the local coordinate system consists of the **equatorial angle** ξ and the **latitudinal angle** η .

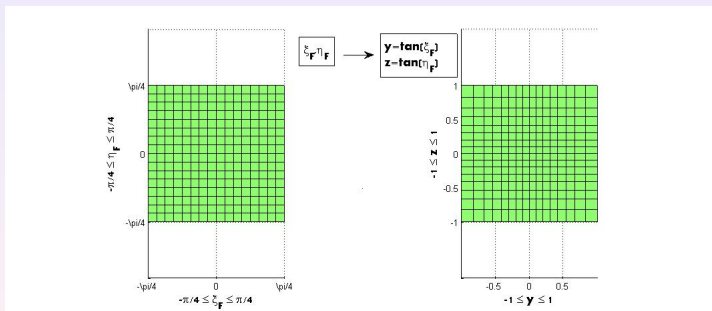


Figure: **Left:** Regular cartesian grid using (ξ_F, η_F) coordinates of the patch FRONT. **Right:** Projection of the Grid onto the FRONT face of the cube in the plane $x = 1$.

Six local non-orthogonal coordinate systems

- The metric tensor is full

$$G = \frac{1}{\delta^4}(1 + X^2)(1 + Y^2) \begin{bmatrix} 1 + X^2 & -XY \\ -XY & 1 + Y^2 \end{bmatrix}, \quad (1)$$

$X = \tan(\xi)$, $Y = \tan(\eta)$ are the **gnomonic coordinates**, image of the (ξ, η) coordinates on the faces of the cube, and $\delta = \sqrt{1 + X^2 + Y^2}$.

- The covariant and contravariant local bases (g_ξ, g_η) and (g^ξ, g^η) have a simple expression in terms of (X, Y) .

Grid function on the Cubed-Sphere

Discrete data representation

The simplest choice of data representation on the Cubed-Sphere is called a **grid function**. On each cartesian grid I, II, III, IV, V , and VI it consists of point values $v_{i,j}$ (classical finite-differences).

Grid function

A grid function on the Cubed-Sphere consists of the 6 sets of data

$$u_{i,j}^k, \quad -M \leq i, j \leq M, \quad k = I, II, III, IV, V, VI, \quad (2)$$

with $M = N/2$, $N =$ size of the local grid.

Spherical periodicity

The spherical periodicity is expressed as

- Matching the values along the 12 edges.
- Matching the values at the 8 corners.

Three-point Hermitian Derivative Operator

Non-local finite difference derivative

The **Hermitian discrete derivative** of a sequence $(u_j)_{j \in \mathbb{Z}}$ is the sequence $(u_{x,j})_{j \in \mathbb{Z}}$ defined by

$$\sigma_x u_{x,j} = \delta_x u_j, \quad j \in \mathbb{Z}, \quad (3)$$

where σ_x, δ_x are the finite difference operators

$$\underbrace{\frac{1}{6}u_{x,j-1} + \frac{2}{3}u_{x,j} + \frac{1}{6}u_{x,j+1}}_{\sigma_x u_{x,j}} = \underbrace{\frac{u_{j+1} - u_{j-1}}{2h}}_{\delta_x u_j}, \quad h > 0 \quad (4)$$

Truncation error

The Hermitian derivative is pointwise fourth-order accurate (analog to the pointwise cubic spline derivative),

$$u_{x,j} = u'(x_j) + O(h^4) \quad (5)$$

Hermitian derivative on an irregular periodic grid

Irregular grid

An irregular periodic grid is given by $\alpha_j = \varphi(x_j)$ $0 \leq j \leq N - 1$ with $x_N = x_0$. The grid $x_j = jh$ is an equispaced discretisation of $[0, 1]$ with 1-periodicity.

Discrete chain-rule

The Hermitian derivative $u_{\alpha,j}$ at α_j is defined by

$$u_{\alpha,j} = \frac{(u \circ \varphi)_{x,j}}{\varphi_{x,j}}, \quad 0 \leq j \leq N - 1, \quad (6)$$

where

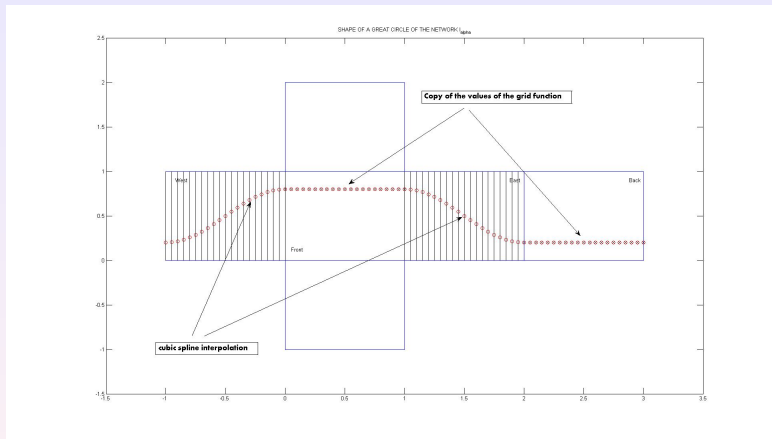
- $\varphi_{x,j}$ is the Hermitian derivative of $\varphi(x)$ at point x_j .
- $(u \circ \varphi)_{x,j}$ is the Hermitian derivative of $(u \circ \varphi)(x)$ at point x_j .

Discrete gradient on the Cubed-Sphere

Calculation principle

- Calculate Hermitian derivatives along great circles (geodesics) of the Cubed-Sphere.
- Reconstruct from a set of suitably selected Hermitian derivatives a fourth-order discrete spherical gradient at each grid point.

Assembling data along great circle coordinate lines of the patches FRONT and BACK



- Figure:**
- Patches FRONT and BACK: copying data.
 - Patches EAST and WEST: interpolating data using cubic splines along iso- ξ lines.

Network I_α of great circles associated to the patches FRONT and BACK

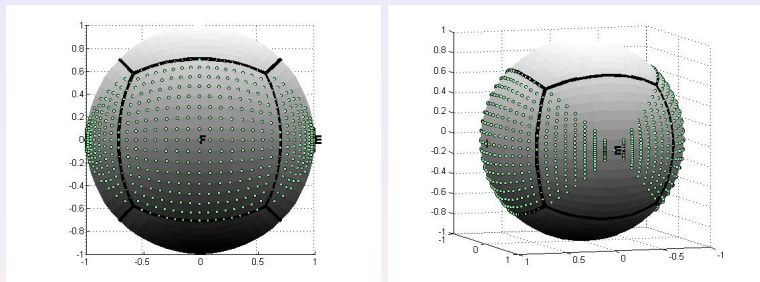


Figure: Network I_α : Iso- η coordinate great circles of patches FRONT and BACK

Network I_β of of great circles associated to the patch FRONT and BACK

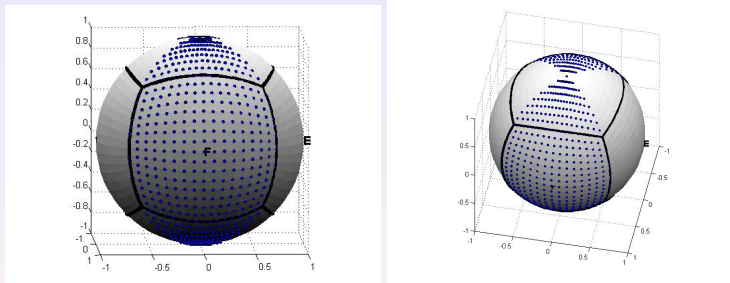


Figure: Network I_β : Iso- ξ coordinate great circles of patches FRONT and BACK

Calculating gradient on patches FRONT and BACK

STEP 1:

Calculating Hermitian derivatives

One-dimensional Hermitian derivatives are computed along great circles of networks I_α and I_β .

“Intrinsic” calculation along geodesics

Hermitian derivatives are calculated with respect to angle $\alpha \in [0, 2\pi[$ (resp. $\beta \in [0, 2\pi[$), which is the curvilinear abscissa along each great circle of network I_α (resp. I_β).

Main observation

This approach avoids dealing with local interpatch treatment to cope with the discontinuity of the metrics.

Calculating gradient on patch FRONT and BACK

STEP 2:

Calculating the discrete spherical gradient

Pointwise evaluation of the discrete gradient $\nabla_s u$ on patches FRONT and BACK using

$$\nabla_s u = \frac{\partial u}{\partial \xi}|_\eta \mathbf{g}^\xi + \frac{\partial u}{\partial \eta}|_\xi \mathbf{g}^\eta, \quad (7)$$

where $(\mathbf{g}^\xi, \mathbf{g}^\eta)$ is the local contravariant basis at (ξ, η) .

Chain rule in one dimension

The partial derivatives $\frac{\partial u}{\partial \xi}|_\eta$ and $\frac{\partial u}{\partial \eta}|_\xi$ are deduced from the Hermitian derivatives using the chain rule as

$$\begin{cases} \frac{\partial u}{\partial \xi}|_\eta = \frac{\partial u}{\partial \alpha}|_\eta \frac{\partial \alpha}{\partial \xi}|_\eta, \\ \frac{\partial u}{\partial \eta}|_\xi = \frac{\partial u}{\partial \beta}|_\xi \frac{\partial \beta}{\partial \eta}|_\xi. \end{cases} \quad (8)$$

Final explicit formula

Spherical gradient on patches FRONT and BACK

$$\begin{aligned} \nabla_{s,h} u_{i,j} &= \underbrace{u_{\alpha,i,j}}_{\alpha\text{-Hermitian deriv.}} \left(\cos \eta_j \frac{1 + \tan^2 \xi_i}{1 + \cos^2 \eta_j \tan^2 \xi_i} \right) \mathbf{g}_{i,j}^{\xi} \\ &+ \underbrace{u_{\beta,i,j}}_{\beta\text{-Hermitian deriv.}} \left(\cos \xi_i \frac{1 + \tan^2 \eta_j}{1 + \cos^2 \xi_i \tan^2 \eta_j} \right) \mathbf{g}_{i,j}^{\eta}. \end{aligned} \quad (9)$$

Full gradient calculation on the Cubed-Sphere

Analog calculations for the pair of patches WEST/EAST and NORTH/SOUTH.

Test 1: Accuracy of the calculated gradient

Approximate gradient of $u(x, y, z) = \sin(10\pi x) \sin(2\pi y) \sin(6\pi z)$

	N=8	rate	N=16	rate	N=32	rate	N=64	rate	N=128
e_∞	23.475	2.99	2.949	4.61	0.121	4.07	7.205(-3)	3.91	4.774(-4)
$\Delta\xi$ in km	1250		625		312.5		156.25		78.12
Nb of grid points	386		1538		6146		24578		93306

Table: Convergence rate of the hermitian gradient of the oscillating function $u(x, y, z) = \sin(10\pi x) \sin(2\pi y) \sin(6\pi z)$ restricted to the unit sphere.

Test 2: Cosine-bell test case (D. Williamson *et al.*)

Advection equation on the sphere

- Test problem : propagation of a cosine-bell at constant solid spherical velocity around the earth.
- Serves as a preliminary test to evaluate the accuracy of numerical methods for the shallow water system
- Reference results widely reported in the literature by various kinds of spatial approximations: spectral, FV MUSCL, SE, DG, etc, on various grids: longitude/latitude, icosahedral, Cubed-Sphere, etc.

Setting of the problem

$h(\mathbf{x}, t)$ = height of the bell.

$$\begin{cases} \partial_t H(\mathbf{x}, t) + \mathbf{c} \cdot \nabla_s H(\mathbf{x}, t) = 0 \\ H(\mathbf{x}, 0) = H_0(\mathbf{x}). \end{cases} \quad (10)$$

The velocity is a “constant” solid velocity.

Spatial approximation

Centered finite-difference scheme

Purpose: assess the accuracy of the new approximate gradient. We thus use the centered semi-discrete fourth-order scheme.

$$\frac{dH_{i,j}^k(t)}{dt} + c \cdot \nabla_{s,h} H_{i,j}^k(t) = 0, \quad -M \leq i, j \leq M, \quad I \leq k \leq VI. \quad (11)$$

Filtering

No upwinding is necessary to handle a linear wave propagation problem. A simple high-frequency filter is enough to damp high-frequency dispersive oscillations of a centered scheme.

Tenth-order filter

Suppression of the numerical dispersive effect supported by the “1/−1” mode. Filtering is a well-known practice in finite-difference computations.

Fourth-order time-stepping scheme

Runge-Kutta RK4 scheme

For the time-dependent system

$$\frac{d}{dt}V(t) = AV(t), \quad A \in \mathbb{M}_N(\mathbb{R}), \quad (12)$$

the standard explicit RK4 scheme is

$$\begin{cases} k_0 = AV^n \\ k_1 = A(V^n + \frac{1}{2}\Delta t k_0) \\ k_2 = A(V^n + \frac{1}{2}\Delta t k_1) \\ k_3 = A(V^n + \Delta t k_2) \\ V^{n+1} = V^n + \Delta t \left(\frac{1}{6}k_0 + \frac{1}{3}k_1 + \frac{1}{3}k_2 + \frac{1}{6}k_3 \right). \end{cases} \quad (13)$$

Cosine-bell test case: numerical results (1)

History of the errors

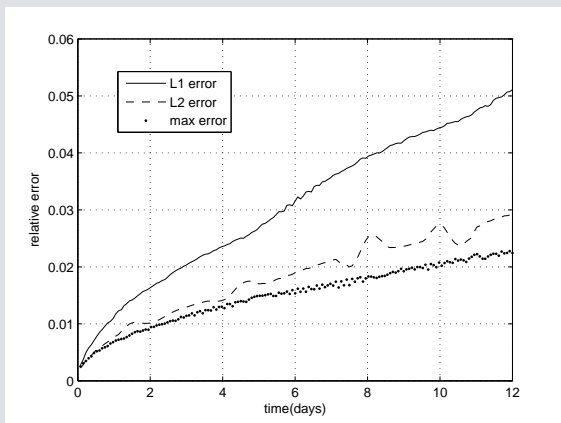


Figure: History of the three relative errors L^1 , L^2 , L^∞ for the cosine-bell advection problem for a cubed-sphere grid of size $N = 40$.

Cosine-bell test case: numerical results (2)

Isolines

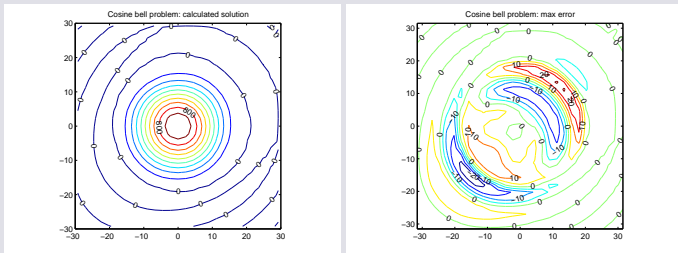


Figure: Contours after one rotation with $\alpha = \pi/4$. Left: numerical solution. Right: error. The cubed-sphere uses $N = 40$. The propagation is oriented towards north-east.

Approximate spherical divergence

Principle

For F a tangential vector field, use on each patch the formula

$$\operatorname{div}_S \mathbf{F} = \frac{1}{\sqrt{G}} \left[\frac{\partial}{\partial \xi} (\sqrt{G} \mathbf{F} \cdot \mathbf{g}^\xi)_{|\eta} + \frac{\partial}{\partial \eta} (\sqrt{G} \mathbf{F} \cdot \mathbf{g}^\eta)_{|\xi} \right] \quad (14)$$

“Intrinsic” calculation using Hermitian derivatives

Calculating the divergence on patches FRONT and BACK using Hermitian derivatives along great circles of the networks I_α and I_β .



$$\frac{\partial}{\partial \xi} (\sqrt{G} \mathbf{F} \cdot \mathbf{g}^\xi)_{|\eta} = \frac{\partial}{\partial \alpha} (\sqrt{G} \mathbf{F} \cdot \mathbf{g}^\xi)_{|\eta} \frac{\partial \alpha}{\partial \xi} \Big|_\eta, \quad (15)$$



$$\frac{\partial}{\partial \eta} (\sqrt{G} \mathbf{F} \cdot \mathbf{g}^\eta)_{|\xi} = \frac{\partial}{\partial \beta} (\sqrt{G} \mathbf{F} \cdot \mathbf{g}^\eta)_{|\xi} \frac{\partial \beta}{\partial \eta} \Big|_\xi. \quad (16)$$

Accuracy of the calculated divergence

Numerical test

Tangential vector functions of the form

$$\mathbf{F} = c(\mathbf{x}) \mathbf{n}(\mathbf{x}) \times \boldsymbol{\phi}, \quad \operatorname{div}_S \mathbf{F} = \nabla_S c(\mathbf{x}) \cdot \mathbf{n}(\mathbf{x}) \times \boldsymbol{\phi}$$

	N=8	rate	N=16	rate	N=32	rate	N=64	rate	N=128
e_∞	33.064(0)	3.83	2.321(0)	4.42	1.087(-1)	4.10	6.311(-3)	4.02	3.870(-4)
$\Delta\xi$ in km	1250		625		312.5		156.25		78.12
Nb of grid points	386		1538		6146		24578		93306

Table: Error between the calculated and the exact spherical divergence.

$$c(\mathbf{x}) = \sin(4\pi x) + \sin(\pi y) + \sin(6\pi z), \quad \boldsymbol{\phi} = [1, 1, 1]^T.$$

Further observations and future work

Higher-order accuracy

Higher-order accuracy achievable using higher-order Hermitian derivatives.

Fast computing issues

Using fast computing tools such as local FFT seems attractive. Useful for implicit time-stepping schemes.

Wave problems on the Cubed-Sphere

Centered fourth-order finite-difference schemes for wave problems on the spherical earth. Short term objective: Laplace Tidal Equations.

High-order accurate spherical gradients for the 4th-order MUSCL scheme

Having at hand high-order gradients, Hessians, etc, is a crucial issue for the design of stable fourth-order MUSCL method for the full SW equations on the sphere.